



Contents lists available at ScienceDirect

Journal of King Saud University – Science

journal homepage: [www.sciencedirect.com](http://www.sciencedirect.com)

# Oxidation of graphene via a simplified Hummers' method for graphene-diamine colloid production

Muhammad Helmi Abdul Kudus<sup>a</sup>, Muhammad Razlan Zakaria<sup>a</sup>, Hazizan Md. Akil<sup>a,\*</sup>, Faheem Ullah<sup>a</sup>, Fatima Javed<sup>b</sup>

<sup>a</sup>School of Materials and Minerals Resources Engineering, Engineering Campus, Universiti Sains Malaysia, 14300 Nibong Tebal, Pulau Pinang, Malaysia

<sup>b</sup>Department of Chemistry, Shaheed Benazir Bhutto Women University, Peshawar, KPK, Pakistan

## ARTICLE INFO

### Article history:

Received 12 March 2019

Revised 28 April 2019

Accepted 15 May 2019

Available online 15 May 2019

### Keywords:

Carbon materials

Nanocomposites

Functional

Colloidal processing

Composite materials

## ABSTRACT

Graphene oxide was prepared by oxidizing the graphene via a simplified Hummers' method, where it had involved the oxidization of the ultrasonically exfoliated water-dispersible graphene in a H<sub>2</sub>SO<sub>4</sub>/HNO<sub>3</sub> mixture and the neutralization effect of NaOH, but without the presence of the KMnO<sub>4</sub> oxidation agent. From the investigations that were conducted on the physiochemical and structural properties of the material under the Raman spectroscopy, Fourier transform infrared spectroscopy (FTIR) and high resolution transmission electron microscopy (HRTEM) techniques, the graphene was found to have been oxidized and its geometrical topology damaged by the use of strong acids. Apart from the SEM images that were used in the morphology comparison of the oxidized and pristine graphene, the XRD results from this experiment had also demonstrated 2θ of the 12.02° as having an interlayer spacing of 0.77 nm. © 2019 The Authors. Production and hosting by Elsevier B.V. on behalf of King Saud University. This is an open access article under the CC BY-NC-ND license (<http://creativecommons.org/licenses/by-nc-nd/4.0/>).

## 1. Introduction

Graphene has been receiving a widespread attention in the recent years owing to its extraordinary mechanical, electrical and thermal properties and its potential usage in various science and technological applications (Geim and Novoselov, 2007; Yin et al., 2018; Kirubasankar et al., 2018; Zhang et al., 2019; Tian et al., 2019; Le et al., 2019; Gong et al., 2019; Wang et al., 2017; Wang et al., 2018). Graphene is known to possess an enormous specific surface area (2620 m<sup>2</sup> g<sup>-1</sup>), excellent mechanical properties (Young's modulus of 1 TPa and intrinsic strength of 130 GPa), very high electronic conductivity (room-temperature electron mobility of 2.5 × 10<sup>5</sup> cm<sup>2</sup> V<sup>-1</sup> s<sup>-1</sup>) as well as exceptionally high thermal conductivity (above 3000 W m K<sup>-1</sup>), which can be produced by either the mechanical exfoliation of bulk graphite (Novoselov et al., 2004) or epitaxial chemical vapour deposition (Berger et al., 2006). The water-soluble derivative of graphene, graphene

oxide, is also a highly prized material that is being used extensively in various applications (Zhu et al., 2010; Bao et al., 2011). Unlike graphene, graphene oxide is a non-conductive hydrophilic carbon material that relies heavily on its degree of oxidation, which can be produced by either the top-down or bottom-up methods, where in the former, the graphene oxide is obtained from the electrochemical exfoliations of the graphite and the latter involving the chemical production of graphene oxide from the readily synthesized graphene. Despite the rare use of the bottom-up method because of the high cost involved, this method however, is still being employed in the production of graphene oxide at the laboratories. Both the Hummers' (Hummers and Offeman, 1958) and modified Hummers' methods (Narasimharao et al., 2016), which are known for using the top-down approach had reported the strong oxidation agent as resulting a medium to high degree of oxidation on the graphene surfaces and edges that will consequently compromise its electrical conductivity. For this reason, the use of graphene oxide was found to have attracted the utilization of functionalized graphene and graphene nanocomposites in advanced applications as seen from the diamine-functionalized graphene (graphene-diamine) that were used in electrical conductive adhesives (Ghaleb et al., 2017), super capacitor electrodes (Song et al., 2017) and epoxy/graphene nanocomposites (Abdul Kudus et al., 2017; Yu et al., 2016). Since certain applications had still required an average hydrophilicity and electrical conductivity levels, this study had therefore proposed combining the Hummers' and

\* Corresponding author.

E-mail address: [hazizan@usm.my](mailto:hazizan@usm.my) (H.Md. Akil).

Peer review under responsibility of King Saud University.



Production and hosting by Elsevier

bottom-up methods, but with the elimination of certain steps and the chemical usage of  $\text{KMnO}_4$  and  $\text{NaNO}_3$  for obtaining a lower oxidation of the graphene oxide.

## 2. Experiment

The oxidized graphene (OG) was obtained by oxidizing the graphene via a simplified Hummer's method, which begins by mixing 1 g of graphene, 30 ml of  $\text{H}_2\text{SO}_4$  (98%) and 10 ml of  $\text{HNO}_3$  (98%) in a 1000 ml volumetric flask that was stirred continuously for 2 h. This was followed by the gradual addition of 100 ml of water and the ensuing rapid increase of temperature to nearly 100 °C. Stirring was once again resumed upon the addition of 200 ml of water into the solution, which was then neutralized with NaOH until a pH 7 is observed. After rinsing with deionized (DI) water for five times, the mixture was subsequently subjected to the filtration and oven drying processes. The resulted oxidized graphene (OG) that had existed in powder form was then investigated under the Fourier-transform infrared spectroscopy (FTIR), Raman spectroscopy and high resolution transmission electron microscopy (HRTEM), while the obtained OG (0.5 g) that was used in the colloidal polymerization with TMD (10 g) was found to have formed a stable colloid after a duration of between 5 and 10 min.

## 3. Results and discussion

In the simplified Hummers' method, this technique had utilized the bottom-up approach with the readily synthesized graphene oxidized from a strong acid reaction. Once the mechanical exfoliation of the graphene had been completed by way of sonication, the strong acid would then inflict damages on the surface by breaking the graphitic structure of the graphene with its heat reaction halted by the NaOH. As for the common modified Hummers' method (Narasimharao et al., 2016), the  $\text{KMnO}_4$  was used as a strong oxidation agent to supply the oxygen element, while the nitrate from the  $\text{NaNO}_3$ , which had triggered the formation of carbonyl groups during the reaction process, would then increase the interlayer spacing and consequently assists in more oxidation of the basal planes than those of the graphene sheet edges (Roy Chowdhury et al., 2014). As seen from the above, the simplified method had used the oxygen from the environment in halting the reaction process instead of the  $\text{H}_2\text{O}_2$ , while the addition of NaOH had formed the nitrate salt of  $\text{NaNO}_3$  from the NaOH and  $\text{HNO}_3$  reaction. As a result, the minute oxidation that was formed on the graphene surface from the carbonyl formation of the  $\text{NaNO}_3$

was found to have experienced a gradual cessation because of the titrated NaOH.

### 3.1. Raman spectroscopy

From the Raman spectra of the (a) pristine and (b) oxidized graphenes shown in Fig. 1, peaks at  $1338\text{ cm}^{-1}$  (D band),  $1580\text{ cm}^{-1}$  (G band) and  $2683\text{ cm}^{-1}$  (2D band) were observed from the Raman shift of a pristine graphene, while those of an oxidized graphene had demonstrated peaks at  $1334\text{ cm}^{-1}$  (D band),  $1582\text{ cm}^{-1}$  (G band) and  $2684\text{ cm}^{-1}$  (2D band).

The Raman intensities of both samples as well as the band ratios intensities between the pristine and oxidized graphenes are depicted in Table 1. Since the intensity ratio ( $I_D/I_G$ ) is typically used to investigate the amount of structural defects and disorders (Abdul Kudus et al., 2017), the higher  $I_D/I_G$  ratio that was observed in the oxidized graphene in Table 1 had thus indicated the sample as possessing a higher amount of functional groups as demonstrated by its higher D intensity level (Maktedar et al., 2014). The occurrence of defects on the oxidized graphene from the concentrated acid was found to have given rise to apertures and the formation of epoxide, hydroxyl and carboxyl functional groups on the graphene surface during the oxidation process, which could be explained by the formation of covalent bonds between the functional groups on the basal plane and those of the graphene edges.

### 3.2. Morphology

The morphologies of the pristine and oxidized graphene as revealed by the HRTEM images in Fig. 2 had shown the (a) pristine graphene as having no structural defects and the (b) oxidized graphene with damaged spots on its basal plane.

### 3.3. F-TIR analysis

From the F-TIR analysis of the spectra peaks shown in Fig. 3a, the spectra of the oxidized graphene was found to have demonstrated a broad peak at  $\sim 3500\text{ cm}^{-1}$  hence, indicating that there had been more of  $-\text{OH}$  or  $-\text{COOH}$  groups being formed on the graphene surface as well as its edges as compared to the narrower peak of the non-oxidized GNP at the same wavelength number. The differences of the  $-\text{OH}$  stretching between the pristine and the oxidized graphene spectra had also supported the graphene's successful oxidation from the simplified Hummers' method. As a small amount of nitrate had been intentionally applied to reduce

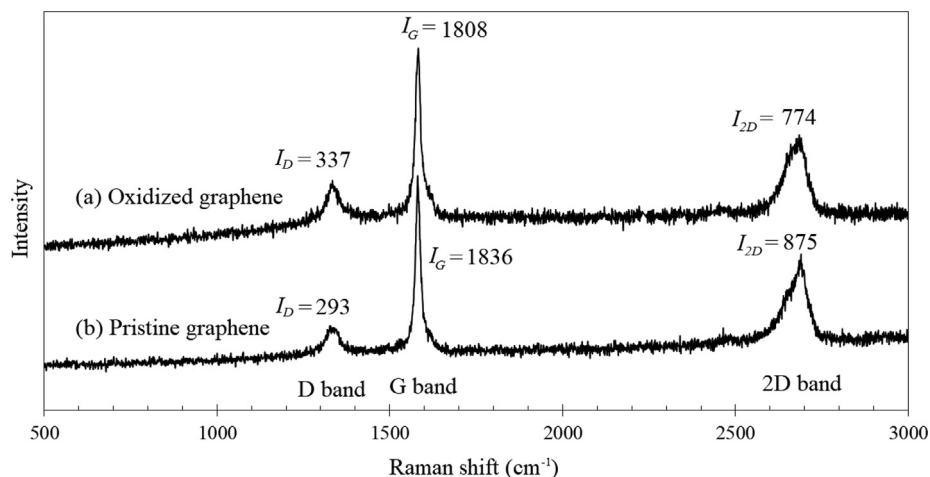
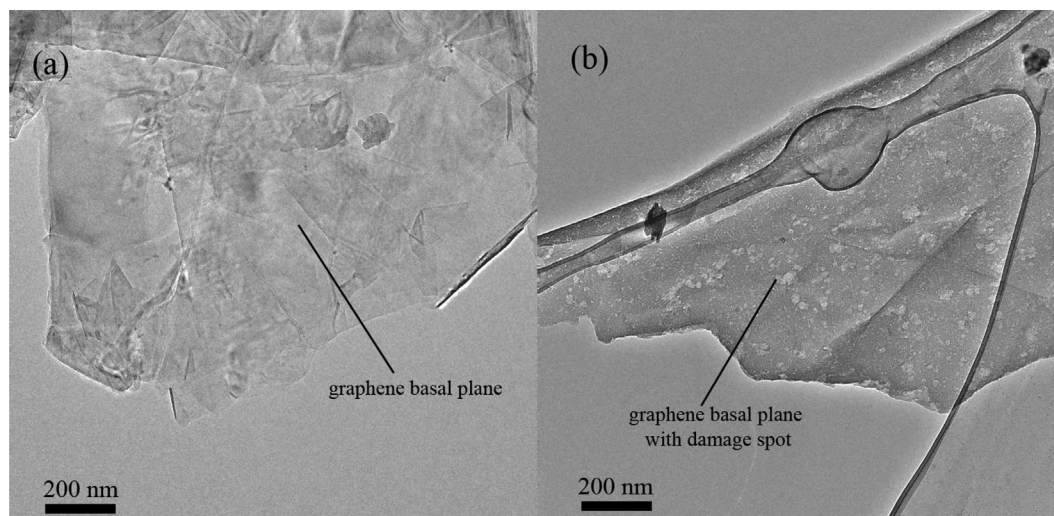


Fig. 1. Raman spectra of (a) oxidized graphene, and (b) pristine graphene.

**Table 1**  
Raman intensity of oxidized graphene and pristine graphene.

Intensity	D band	G band	2D band	$I_D/I_G$	$I_{2D}/I_G$
Oxidized graphene	337	1808	774	0.19	0.43
Pristine graphene	293	1836	875	0.16	0.47



**Fig. 2.** HRTEM images of (a) pristine graphene, and (b) oxidized graphene.

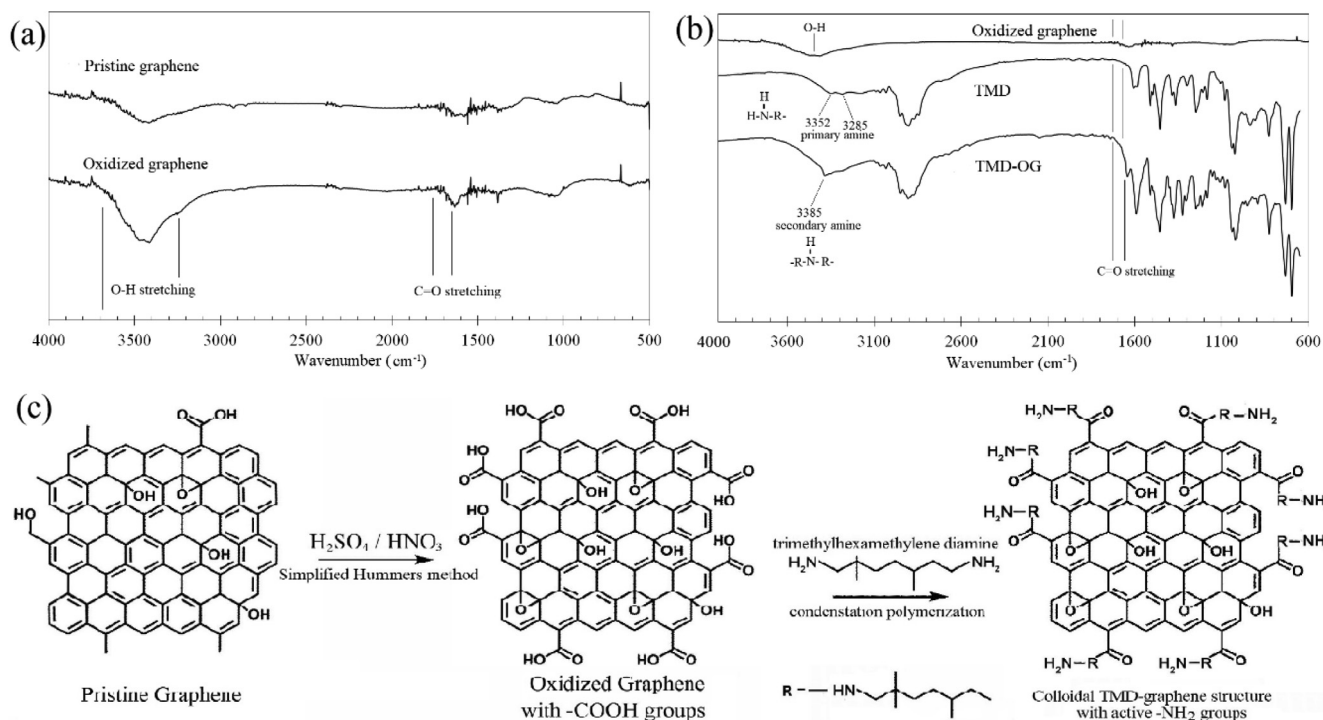


**Fig. 3.** FTIR spectra of (a) pristine graphene and OG; and (b) OG, TMD, and colloid of TMD-OG; and (c) schematic representative of colloidal polymerization mechanism.

the possible damages on the graphene's basal plane, the small changes that were observed on the carbonyl stretching ( $C=O$ ) had therefore indicated the small degree of carboxyl group formation as being related to the presence of nitrate ( $NaNO_3$ ) that was resulted from the NaOH titration process.

### 3.4. Colloidal polymerization

The success of graphene oxidation can be further assessed by examining the reaction of the obtained functional groups with other reactive chemicals, such as those of diamine molecules.

The rapid formation of the stabilised colloid as shown by the dispersed oxidized graphene in the TMD via a high frequency sonication technique had thus implied the occurrence of polymerization between those of the TMD amine groups ( $-NH_2$ ) and the oxidized graphene carboxyl groups ( $-COOH$ ), which could be further validated by the FTIR spectra of the raw TMD and the TMD-OG colloid mixture (as shown in Fig. 3b). Alternatively, the specific reaction of colloidal polymerization between the hydroxyl and diamine groups could also be verified by focusing on the emergence of the amine group, which had occurred at the two spectra peaks of between the 3352 and 3285  $cm^{-1}$  wavelength numbers on the TMD spectrum and the secondary amine of a single peak (3385  $cm^{-1}$ ) on the TMD-OG spectrum. Since the successful graphene oxidation from the simplified Hummers' method was also validated by the schematic diagram of the TMD and OG polymerization reaction as shown in Fig. 3c, this therefore implies that the graphene-diamine colloid has the potential to be used in electronic applications as well as those of epoxy polymer composites.

#### 4. Conclusion

The simplified Hummers' method was not only found to have successfully produced the oxidized graphene without the use of a strong oxidation agent, but the small degree of oxidation had also kept its structural integrity without compromising its thermal and electrical properties. The oxidized graphene and diamine-functionalized graphene were also successfully characterized and confirmed by the respective Raman spectroscopy, FTIR and HRTEM techniques.

#### Acknowledgement

The authors would like to acknowledge Universiti Sains Malaysia (USM) RUI 1001/PBAHAN/8014047 for sponsoring and providing financial assistance during this research work.

#### References

- Abdul Kudus, M.H., Zakaria, M.R., Hafi Othman, M.B., Md Akil, H., 2017. Preparation and characterization of colloidal diamine/oxidized-graphene via condensation polymerization of carboxyl groups epoxy/oxidized-graphene nanocomposite. *Polymer* 124, 186–202.
- Bao, C., Guo, Y., Song, L., Kan, Y., Qian, X., Hu, Y., 2011. In situ preparation of functionalized graphene oxide/epoxy nanocomposites with effective reinforcements. *J. Mater. Chem.* 21 (35), 13290–13298.
- Berger, C., Song, Z., Li, X., Wu, X., Brown, N., Naud, C., Mayou, D., Li, T., Hass, J., Marchenkov, A.N., 2006. Electronic confinement and coherence in patterned epitaxial graphene. *Science* 312 (5777), 1191–1196.
- Geim, A.K., Novoselov, K.S., 2007. The rise of graphene. *Nat. Mater.* 6 (3), 183–191.
- Ghaleb, Z.A., Mariatti, M., Ariff, Z.M., Ervina, J., 2017. Preparation and properties of amine functionalized graphene filled epoxy thin film nano composites for electrically conductive adhesive. *J. Mater. Sci.: Mater. Electron.*
- Gong, X., Liu, Y., Wang, Y., Xie, Z., Dong, Q., Dong, M., Liu, H., Shao, Q., Lu, N., Murugadoss, V., 2019. Amino graphene oxide/dopamine modified aramid fibers: preparation, epoxy nanocomposites and property analysis. *Polymer* 168, 131–137.
- Hummers Jr, W.S., Offeman, R.E., 1958. Preparation of graphitic oxide. *J. Am. Chem. Soc.* 80 (6), 1339.
- Kirubasankar, B., Murugadoss, V., Lin, J., Ding, T., Dong, M., Liu, H., Zhang, J., Li, T., Wang, N., Guo, Z., 2018. In situ grown nickel selenide on graphene nanohybrid electrodes for high energy density asymmetric supercapacitors. *Nanoscale* 10 (43), 20414–20425.
- Le, K., Wang, Z., Wang, F., Wang, Q., Shao, Q., Murugadoss, V., Liu, W., Liu, J., Gao, Q., Wu, S., 2019. Sandwich-like NiCo layered double hydroxides/reduced graphene oxide nanocomposite cathode for high energy density asymmetric supercapacitors. *Dalton Trans.*
- Maktedar, S.S., Mehetre, S.S., Singh, M., Kale, R., 2014. Ultrasound irradiation: a robust approach for direct functionalization of graphene oxide with thermal and antimicrobial aspects. *Ultrason. Sonochem.* 21 (4), 1407–1416.
- Narasimharao, K., Venkata Ramana, G., Sreedhar, D., Vasudevarao, V., 2016. Synthesis of graphene oxide by modified hummers method and hydrothermal synthesis of graphene-nio nano composite for supercapacitor application. *J. Mater. Sci. Eng.* 5 (284), 2169-0022.1000284.
- Novoselov, K.S., Geim, A.K., Morozov, S.V., Jiang, D., Zhang, Y., Dubonos, S.V., Grigorieva, I.V., Firsov, A.A., 2004. Electric field effect in atomically thin carbon films. *Science* 306 (5696), 666–669.
- Roy Chowdhury, D., Singh, C., Paul, A., 2014. Role of graphite precursor and sodium nitrate in graphite oxide synthesis. *RSC Adv.* 4 (29), 15138–15145.
- Song, B., Zhao, J., Wang, M., Mullavey, J., Zhu, Y., Geng, Z., Chen, D., Ding, Y., Moon, K.-S., Liu, M., Wong, C.-P., 2017. Systematic study on structural and electronic properties of diamine/triamine functionalized graphene networks for supercapacitor application. *Nano Energy* 31 (Suppl. C), 183–193.
- Tian, Y., Yang, X., Nautiyal, A., Zheng, Y., Guo, Q., Luo, J., Zhang, X., 2019. One-step microwave synthesis of  $MoS_2/MoO_3@$  graphite nanocomposite as an excellent electrode material for supercapacitors. *Adv. Compos. Hybrid Mater.*, 1–11
- Wang, Z., Wei, R., Gu, J., Liu, H., Liu, C., Luo, C., Kong, J., Shao, Q., Wang, N., Guo, Z., 2018. Ultralight, highly compressible and fire-retardant graphene aerogel with self-adjustable electromagnetic wave absorption. *Carbon* 139, 1126–1135.
- Wang, C., Zhao, M., Li, J., Yu, J., Sun, S., Ge, S., Guo, X., Xie, F., Jiang, B., Wujcik, E.K., 2017. Silver nanoparticles/graphene oxide decorated carbon fiber synergistic reinforcement in epoxy-based composites. *Polymer* 131, 263–271.
- Yin, Y., Jiang, B., Zhu, X., Meng, L., Huang, Y., 2018. Investigation of thermostability of modified graphene oxide/methylsilicone resin nanocomposites. *Eng. Sci.* 5, 73–78.
- Yu, J.W., Jung, J., Choi, Y.-M., Choi, J.H., Yu, J., Lee, J.K., You, N.-H., Goh, M., 2016. Enhancement of the crosslink density, glass transition temperature, and strength of epoxy resin by using functionalized graphene oxide co-curing agents. *Polym. Chem.* 7 (1), 36–43.
- Zhang, J., Zhang, Z., Jiao, Y., Yang, H., Li, Y., Zhang, J., Gao, P., 2019. The graphene/lanthanum oxide nanocomposites as electrode materials of supercapacitors. *J. Power Sources* 419, 99–105.
- Zhu, Y., Murali, S., Cai, W., Li, X., Suk, J.W., Potts, J.R., Ruoff, R.S., 2010. Graphene and graphene oxide: synthesis, properties, and applications. *Adv. Mater.* 22 (35), 3906–3924.